Magnetic helicity and active filaments

P. Romano, S.L. Guglielmino, F.P. Zuccarello, F. Zuccareelo

INAF – Catania Astrophysical Observatory

University of Catania - Department of Physics and Astronomy

LESIA, Observatoire de Paris

Context

Flux ropes

It is considered crucial in many models of the formation and eruption of filaments.

A **magnetic flux rope** (FR) indicates a particular field topology characterized by a set of magnetic field lines that collectively wrap around a central, axial field line.

Its origin is controversial:
- it is formed below the photosphere (Fan et al., 1998; Gibson et al. 2004)
- it re-forms in corona (Fan 2009; Archontis et al. 2014)

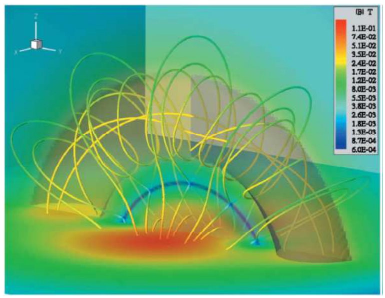

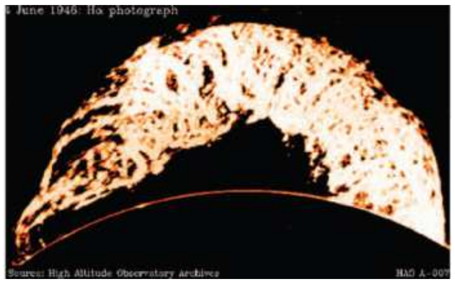

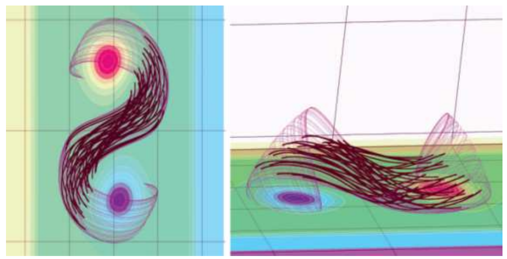

FRs are usually accompained by observations of shearing and rotating motions of magnetic features at photospheric level (Brown et al. 2003)

The sigmoids in EUV and X-ray can be explained with the FR configuration

Context

Magnetic helicity

It may be useful to measure the complexity and instability of the magnetic field in the higher layers of the solar atmosphere by considering the magnetic helicity (H).

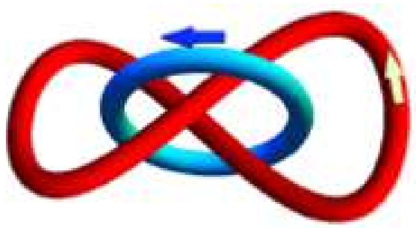

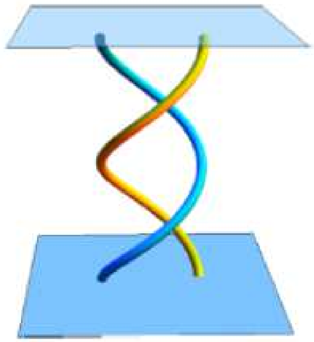

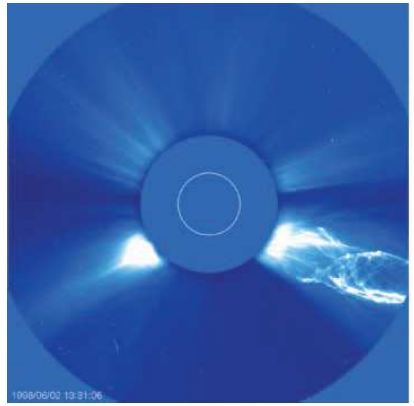

$$H = \int \mathbf{A} \cdot \mathbf{B} \, \mathrm{d}^3 x$$

H is present wherever electric currents are present.

H can generally be treated as conserved in the corona, especially over the timescales of fast reconnection.

Therefore, an isolated helical magnetic structure cannot relax to a potential state unless its magnetic helicity is bodily removed from it (CMEs).

Outline of this work

- Aim:
  - Investigate the trend of magnetic helicity flux during the formation and eruption of flux ropes.

- Targets:
  - **NOAA 11283** (AR hosting recurrent flares of GOES M- and X-class)
  - **NOAA 11318 and NOAA 11675** (two ARs characterized by a completely different magnetic configuration)

- Method:
  - the magnetic helicity trend has been investigated measuring its flux from the convection zone to the corona
  - the photospheric magnetic configuration has been analyzed
  - the evolution of both ARs at different atmospheric levels has been studied

Case 1

Recurrent flares/CMEs
and
monotonic injection of magnetic helicity

Romano et al., A&A, 582, A55, 2015

NOAA 11283

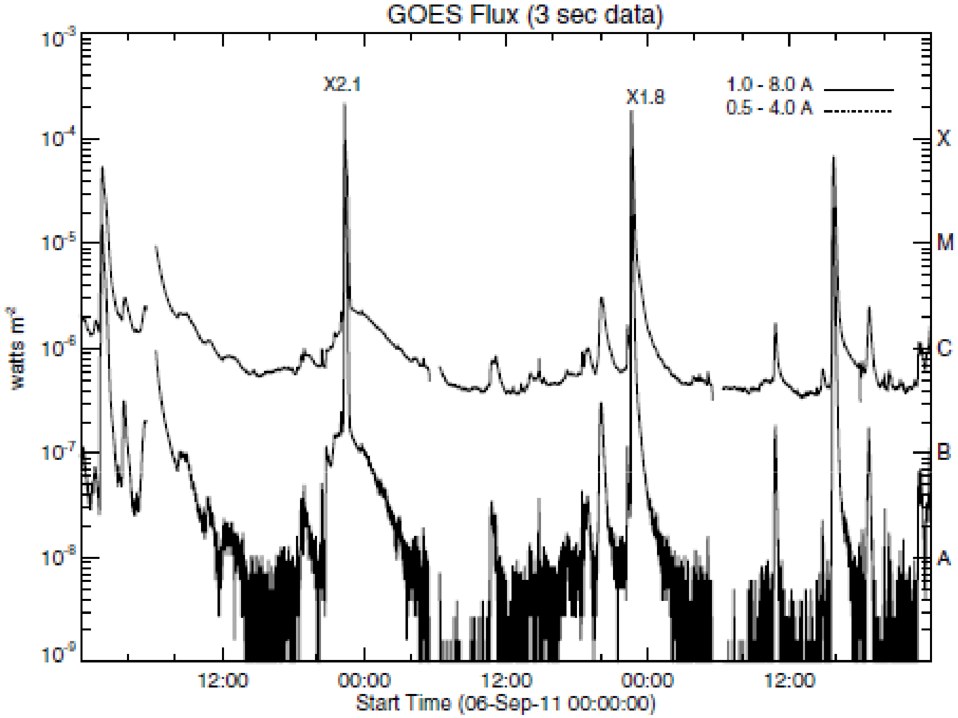

Table 1. M- and X-class flares that occurred in AR NOAA 11283 during the observation interval, as reported by the Space Environment Center.

Date	Start (UT)	Peak (UT)	End (UT)	GOES class
2011-Sept.-6	01:35	01:50	02:05	M5.3
2011-Sept.-6	22:12	22:20	22:24	X2.1
2011-Sept.-7	22:32	22:38	22:44	X1.8
2011-Sept.-8	15:32	15:46	15:52	M6.7

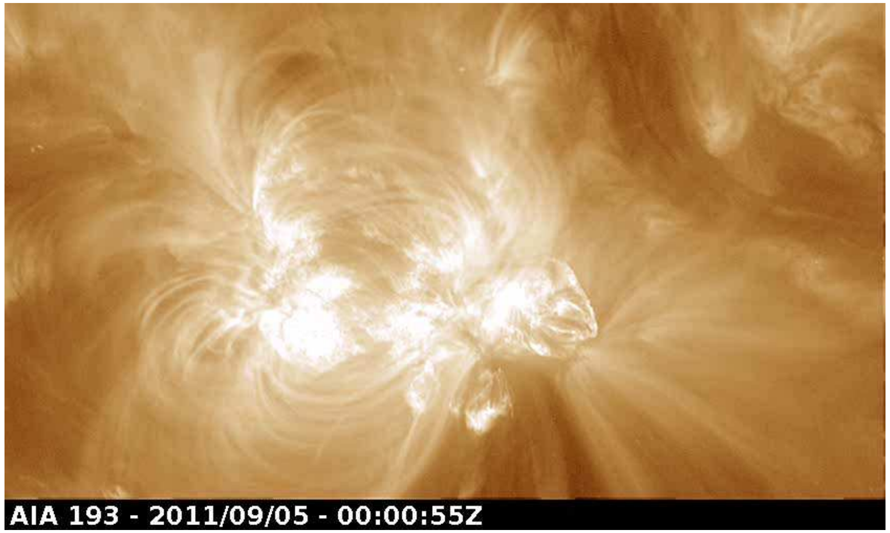

SHARP data (HMI/SDO)

From Sept 5, 2011 at 00:00 UT - Sept 8, at 16:00 UT

Pixel size: 0”.51

Time cadence: 12 min

NOAA 11283

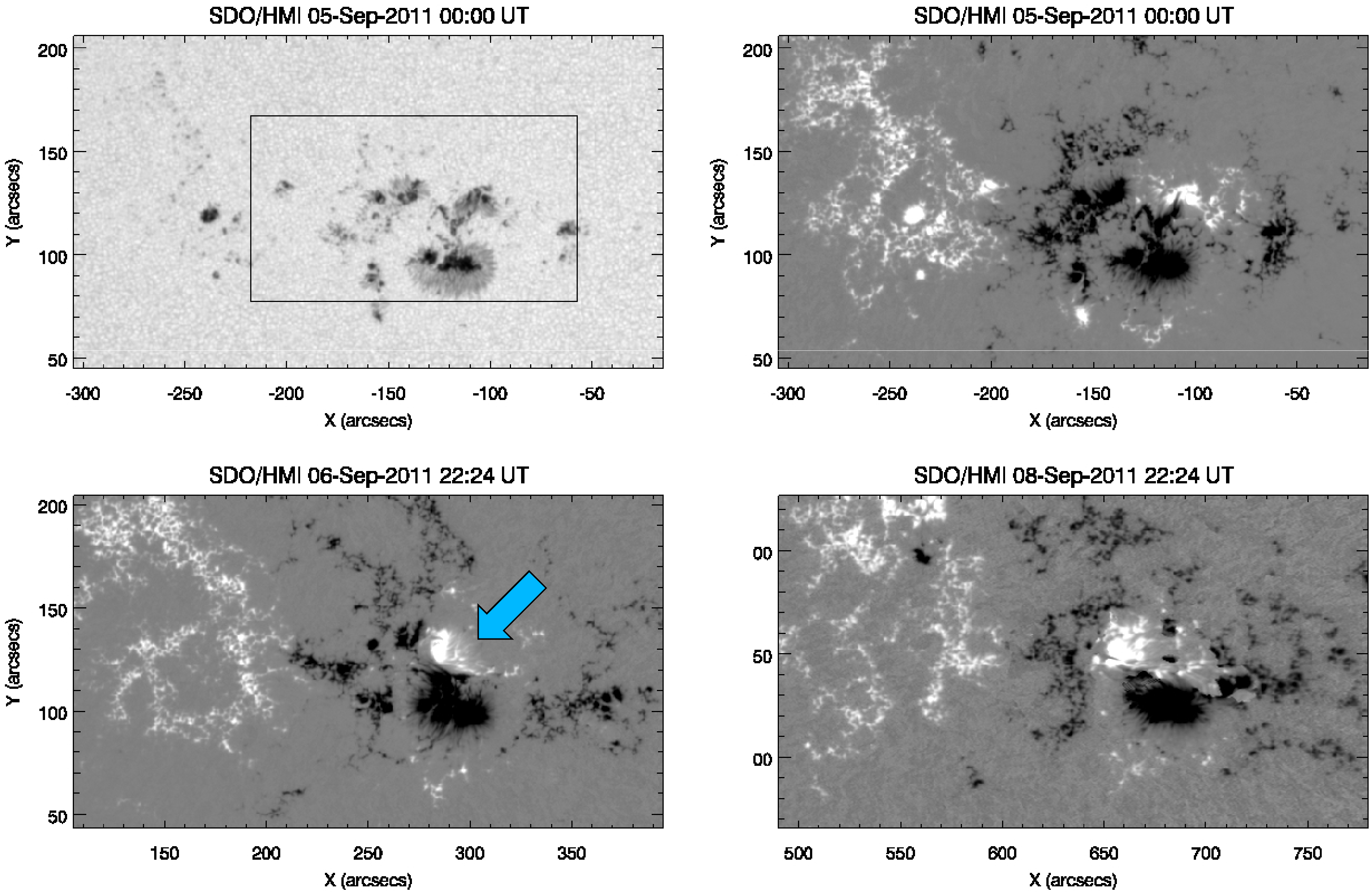
SDO/HMI 05-Sep-2011 00:00 UT
Y (arcsecs)
X (arcsecs)
200
150
100
50
-300
-250
-200
-150
-100
-50
SDO/HMI 05-Sep-2011 00:00 UT
SDO/HMI 06-Sep-2011 22:24 UT
150
200
250
300
350
SDO/HMI 08-Sep-2011 22:24 UT
00
50
500
550
600
650
700
750

NOAA 11283

Shear angle. The shear between the observed (measured) horizontal field and the horizontal field derived through a potential field extrapolation (see Wang et al. 1994).

$$\theta = \arccos \frac{\mathbf{B}_\mathbf{h}^{\mathrm{obs}} \cdot \mathbf{B}_\mathbf{h}^{\mathrm{pot}}}{|B_h^{\mathrm{obs}}||B_h^{\mathrm{pot}}|},$$

Dip angle. It measures the difference between the inclination angle of the observed field and that of the potential field (see, e.g., Gosain & Venkatakrishnan 2010; Petrie 2012).

$$\Delta\gamma = \gamma^{\mathrm{obs}} - \gamma^{\mathrm{pot}},$$

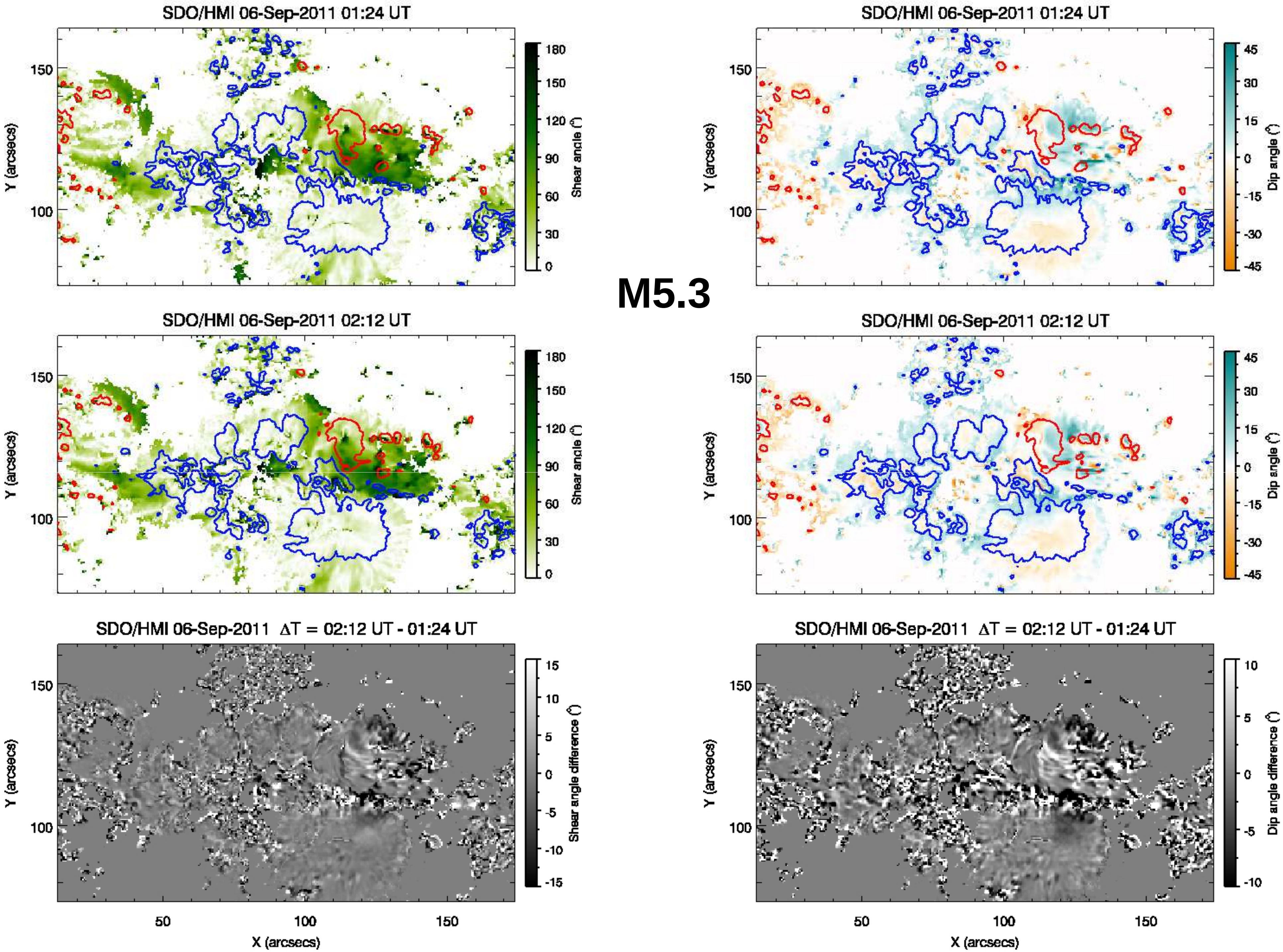

SDO/HMI 06-Sep-2011 01:24 UT
SDO/HMI 06-Sep-2011 01:24 UT
M5.3
SDO/HMI 06-Sep-2011 02:12 UT
SDO/HMI 06-Sep-2011 02:12 UT
SDO/HMI 06-Sep-2011 ΔT = 02:12 UT - 01:24 UT
SDO/HMI 06-Sep-2011 ΔT = 02:12 UT - 01:24 UT
Y (arcsecs)
X (arcsecs)
Shear angle (°)
Dip angle (°)
Shear angle difference (°)
Dip angle difference (°)

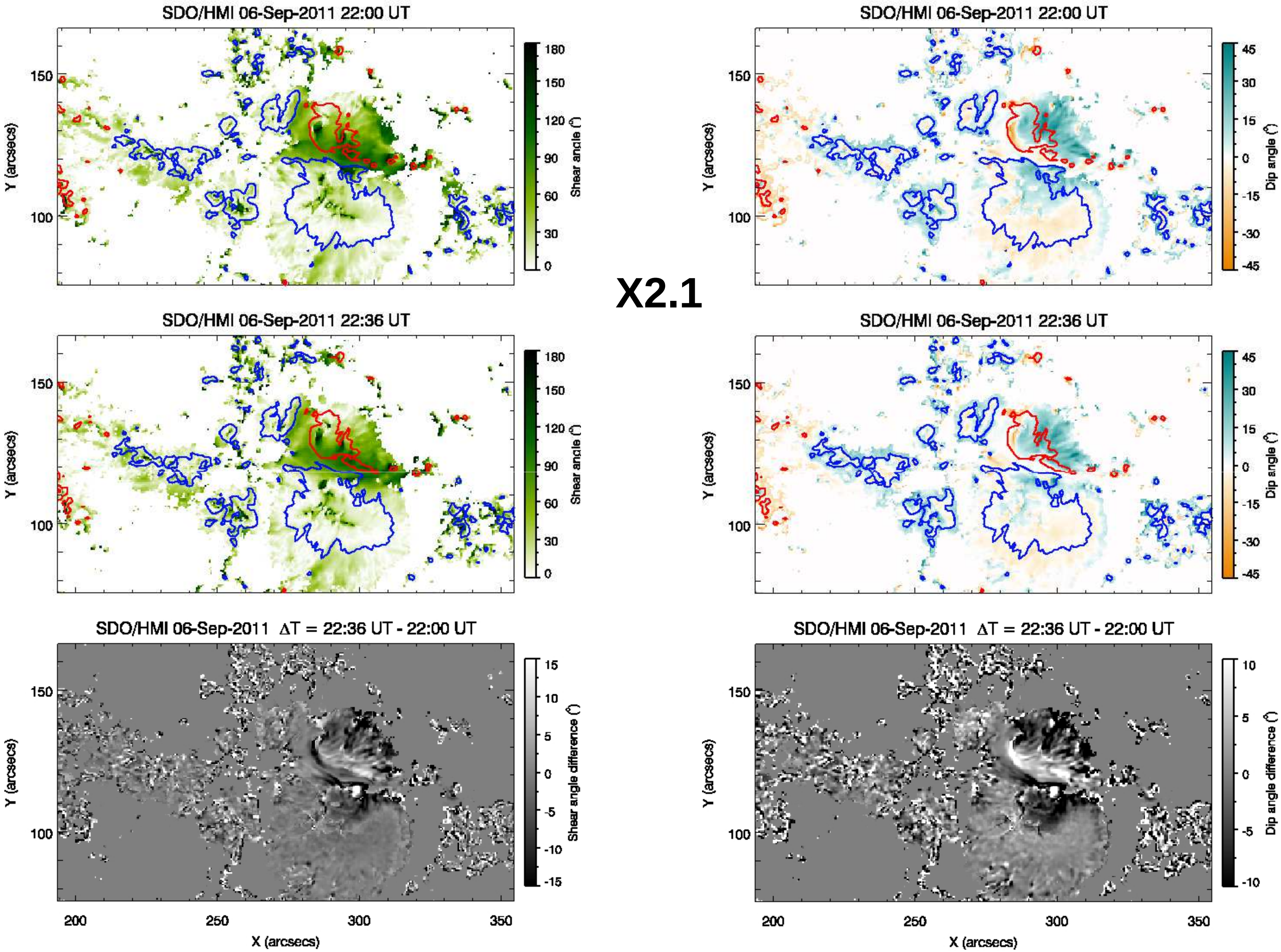

SDO/HMI 06-Sep-2011 22:00 UT
SDO/HMI 06-Sep-2011 22:36 UT
SDO/HMI 06-Sep-2011 ΔT = 22:36 UT - 22:00 UT
Y (arcsecs)
X (arcsecs)
Shear angle (°)
Dip angle (°)
Shear angle difference (°)
Dip angle difference (°)
X2.1

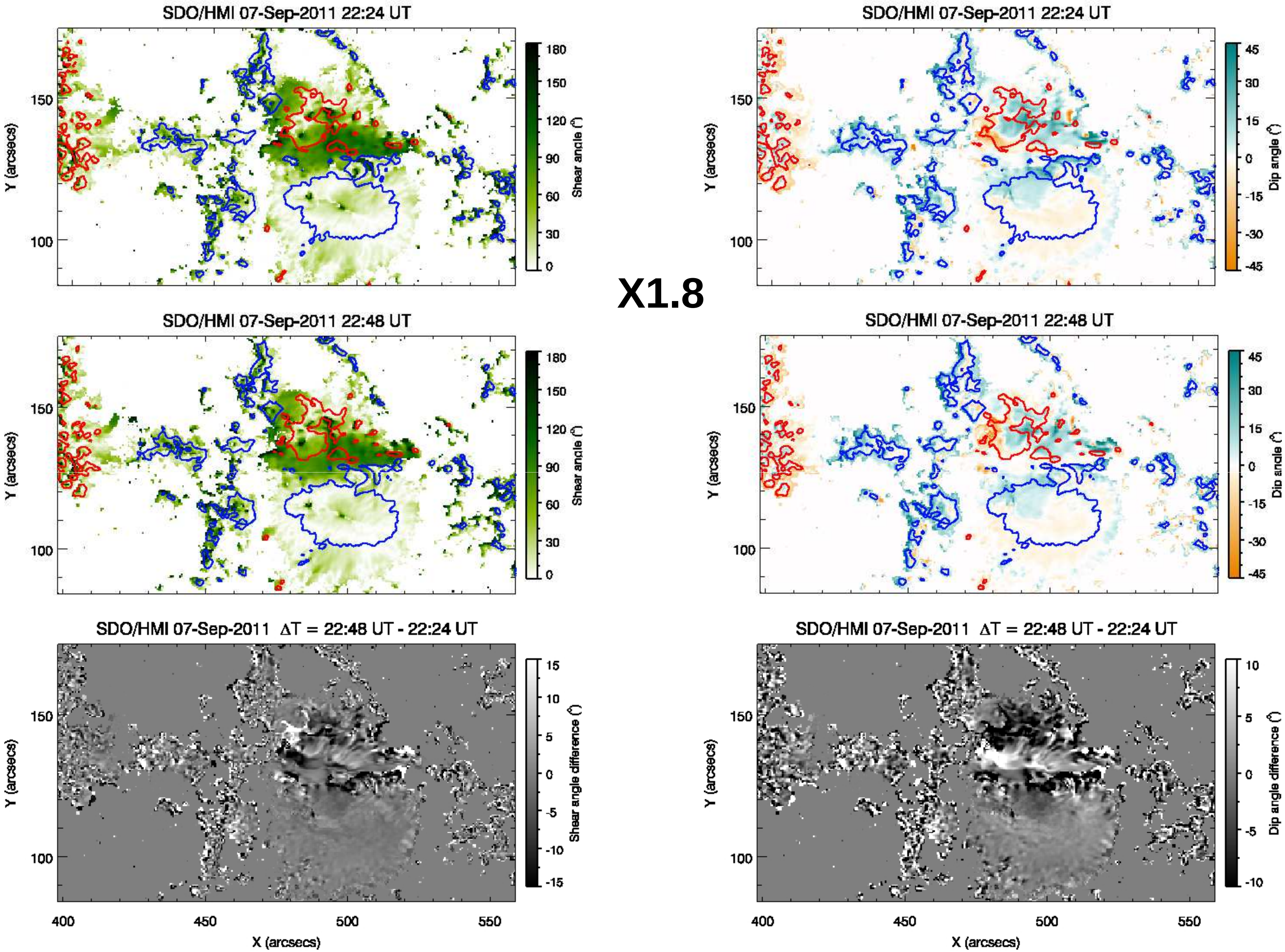

X1.8
SDO/HMI 07-Sep-2011 22:24 UT
SDO/HMI 07-Sep-2011 22:48 UT
SDO/HMI 07-Sep-2011 ΔT = 22:48 UT - 22:24 UT
Shear angle (°)
Dip angle (°)
Shear angle difference (°)
Dip angle difference (°)
X (arcsecs)
Y (arcsecs)

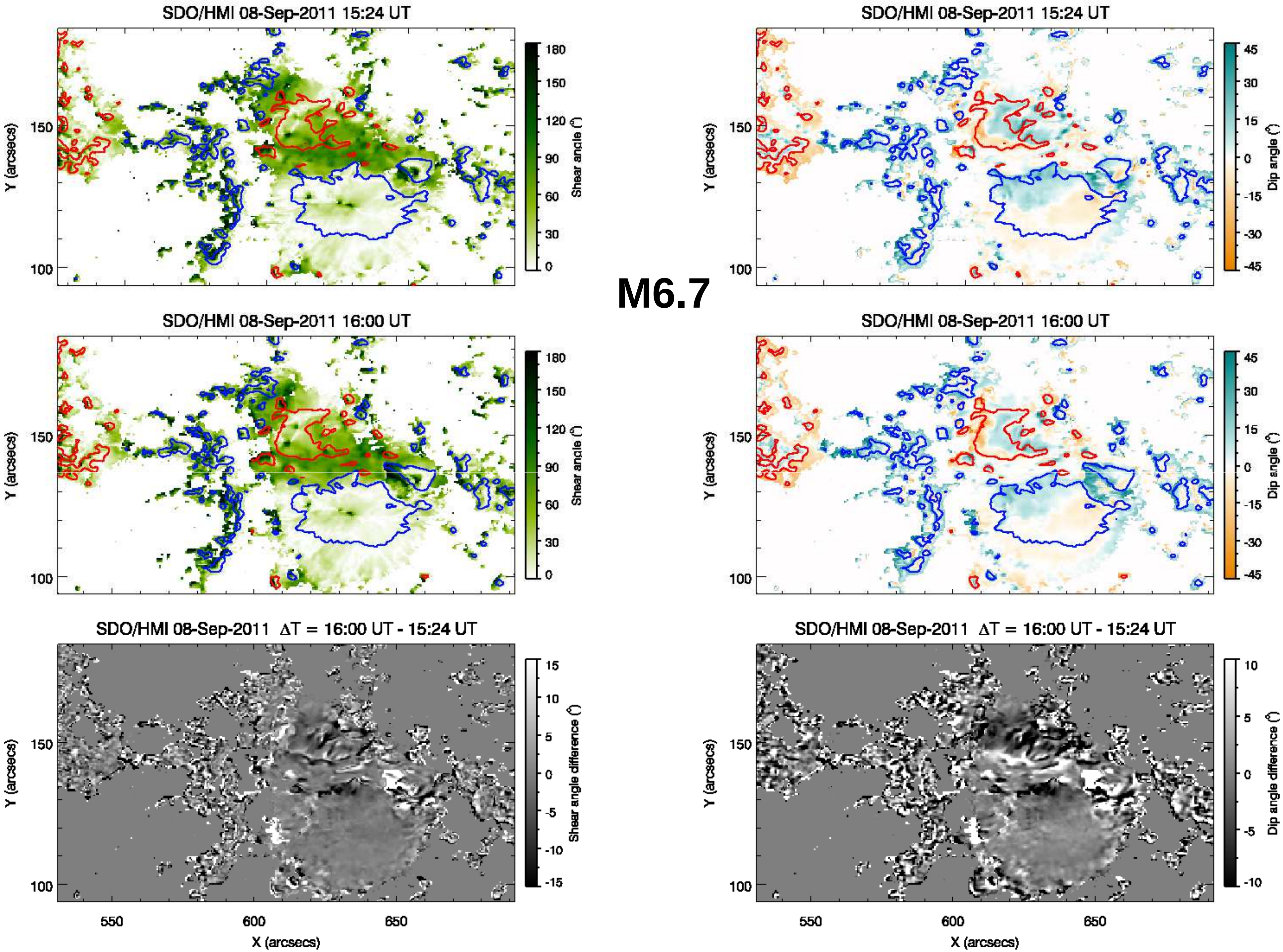
SDO/HMI 08-Sep-2011 15:24 UT
SDO/HMI 08-Sep-2011 16:00 UT
SDO/HMI 08-Sep-2011 ΔT = 16:00 UT - 15:24 UT
M6.7
Y (arcsecs)
X (arcsecs)
Shear angle (°)
Dip angle (°)
Shear angle difference (°)
Dip angle difference (°)
100
150
550
600
650

NOAA 11283

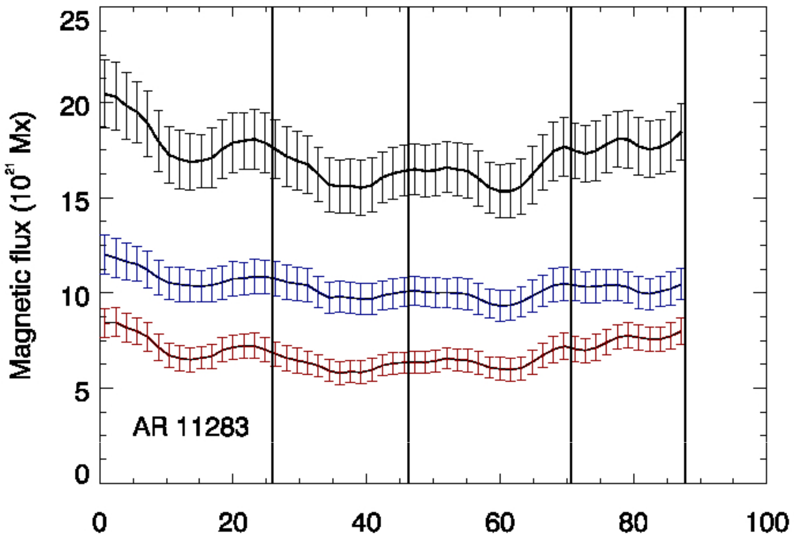
Magnetic flux (10^{21} Mx)
AR 11283

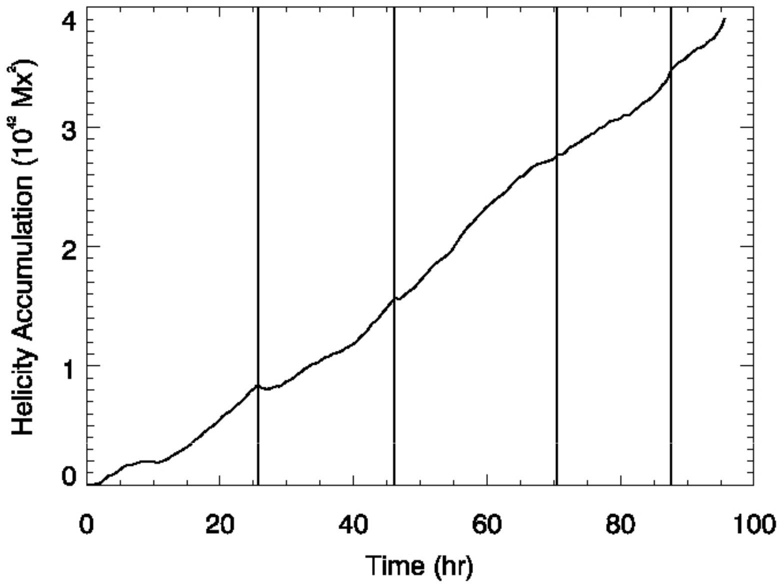
Helicity Accumulation (10^{42} Mx^2)
Time (hr)

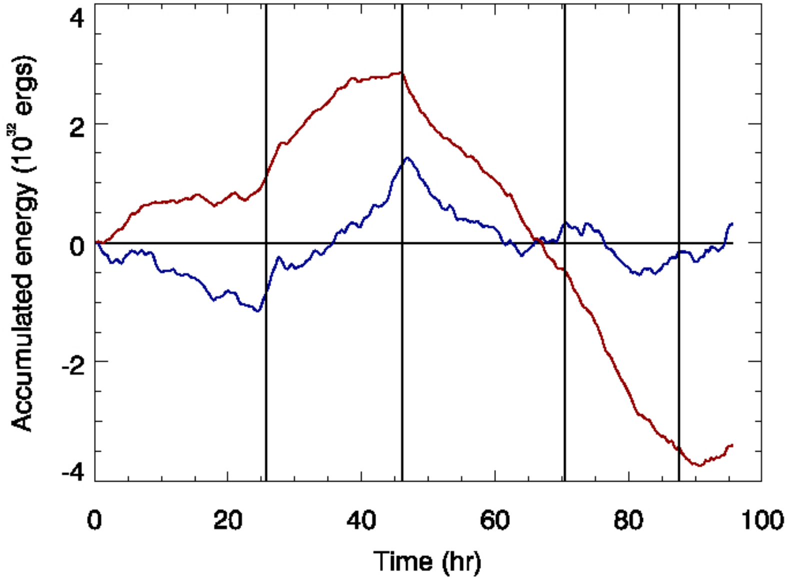
Accumulated energy (10^{32} ergs)
Time (hr)

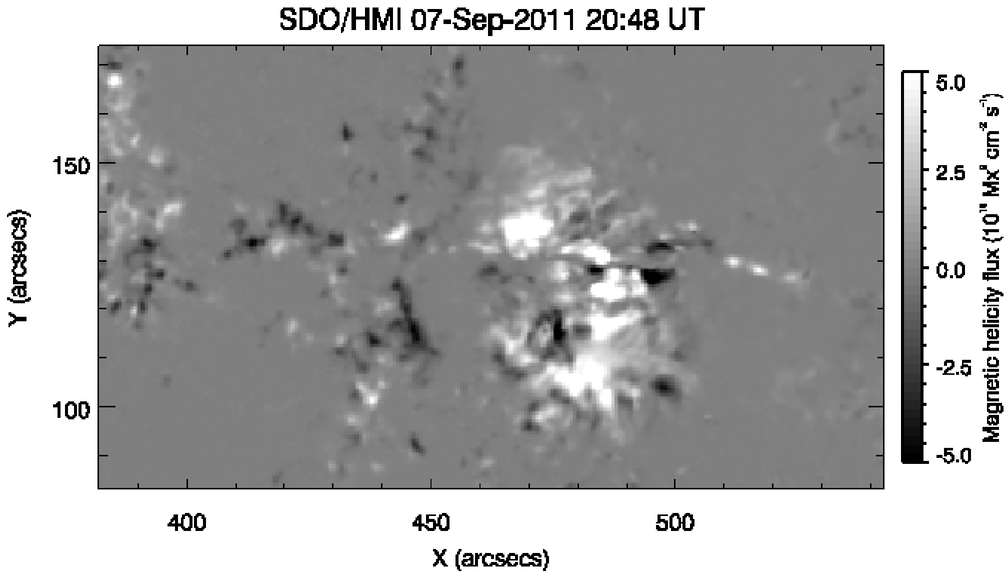
SDO/HMI 07-Sep-2011 20:48 UT
Y (arcsecs)
X (arcsecs)
Magnetic helicity flux (10^{18} Mx^2 cm^{-2} s^{-1})

Case 2

The role of the overlying magnetic field in the confined flares

Romano et al., ApJ, 794, 118, 2014

NOAA 11318

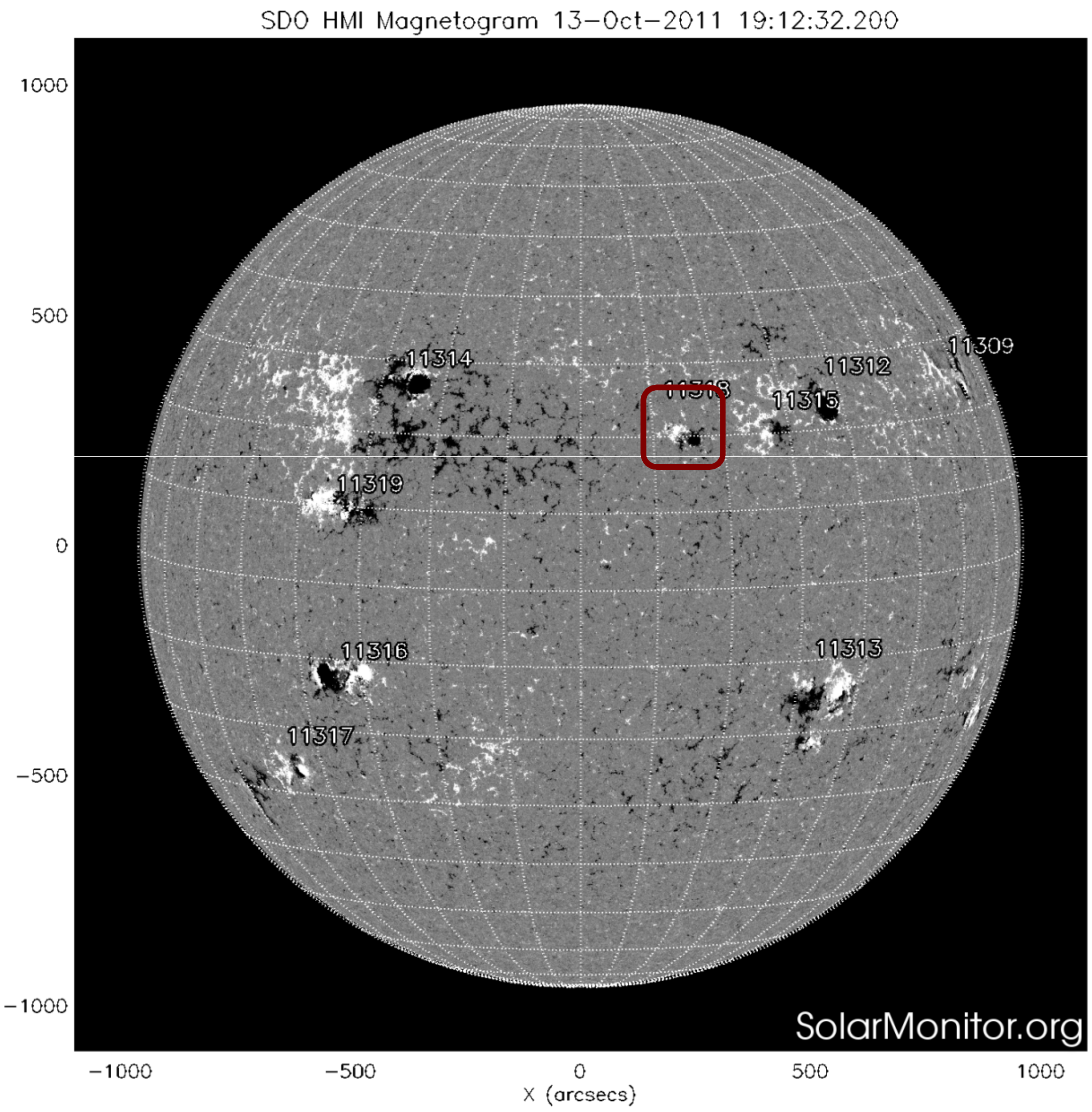

The AR has been studied using AIA/SDO images (171 Å, 193 Å, 304 Å, 335 Å and HMI/SDO longitudinal magnetograms between
11 – 15 Oct 2011

Northern hemisphere (N21)

NOAA 11318: the magnetic field evolution

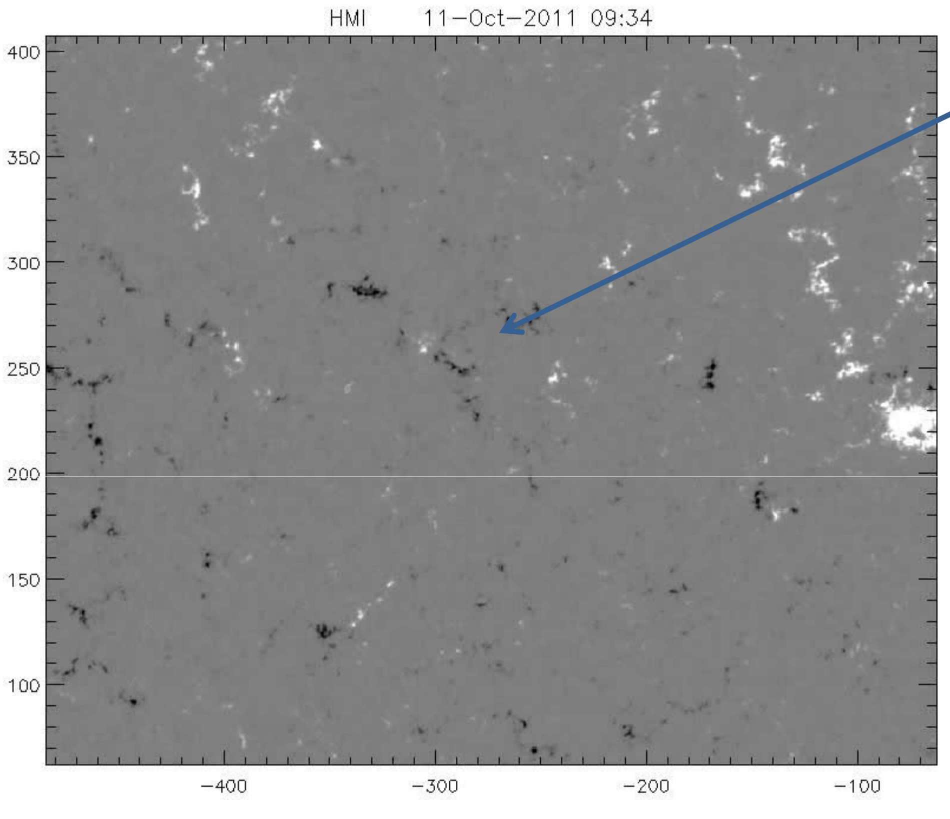

The presence of magnetic tongues can be considered an indication of the appearance of a twisted flux tube (Luoni et al. 2011).

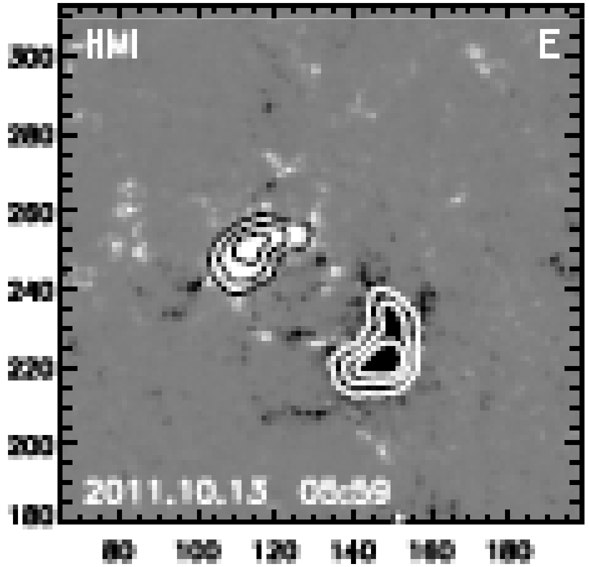

The photospheric magnetic configuration and the continuous separation of the two polarities supports a scenario leading to the appearance of a flux rope.

NOAA 11318 @ 304 Å

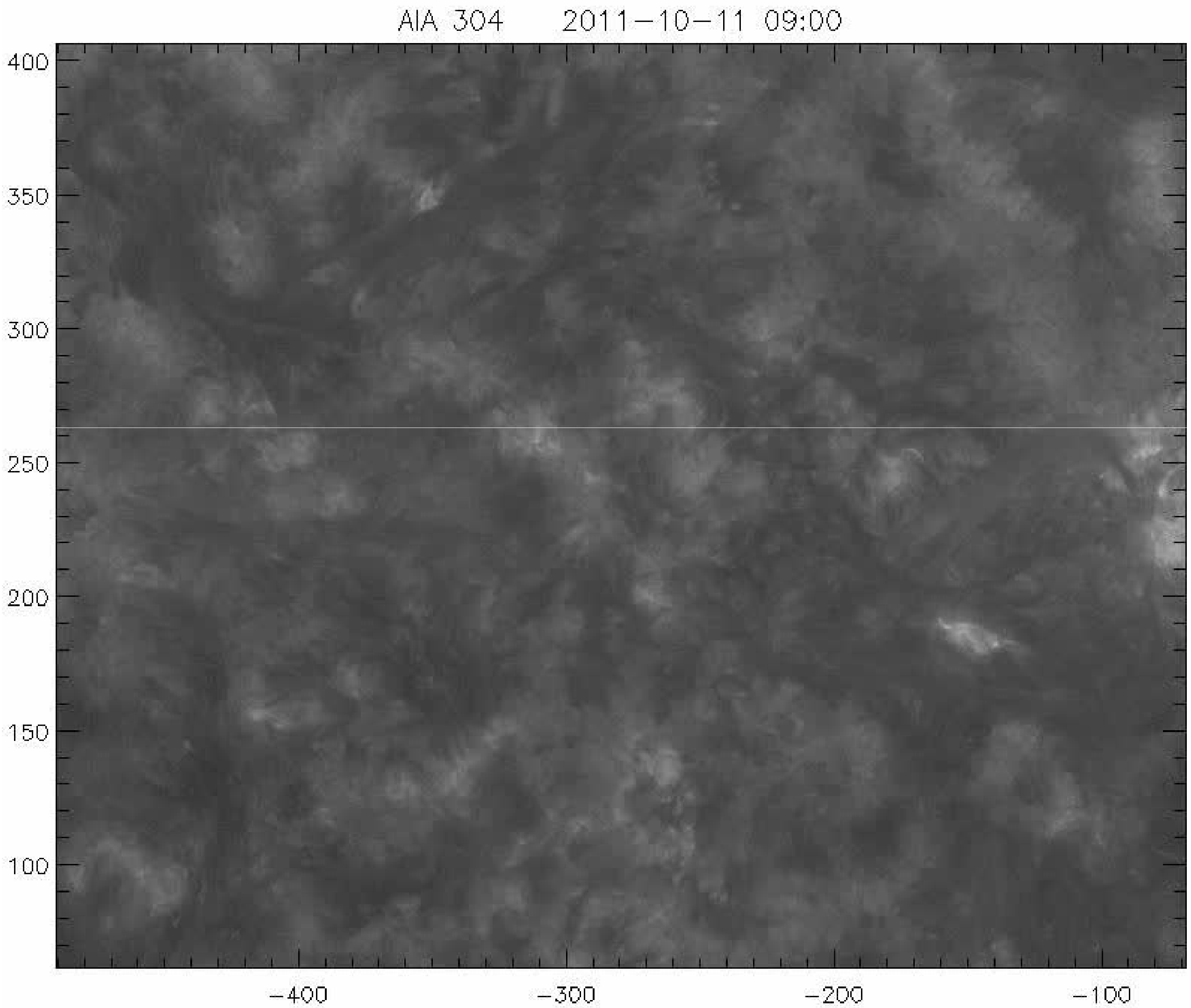

An initial destabilization of a filament is observed at 22:40 UT on 14 Oct and the filament is activated at 02:10 on 15 Oct.

In this case the formation of the FR culminated in a C2.3 class flare observed on 15 Oct 2011 at 04:19 UT (peak 04:40 UT), associated to a **CME** observed by LASCO.

NOAA 11318: the flux rope destabilization and eruption
Note the sigmoid before the flux rope eruption

(193 Å)

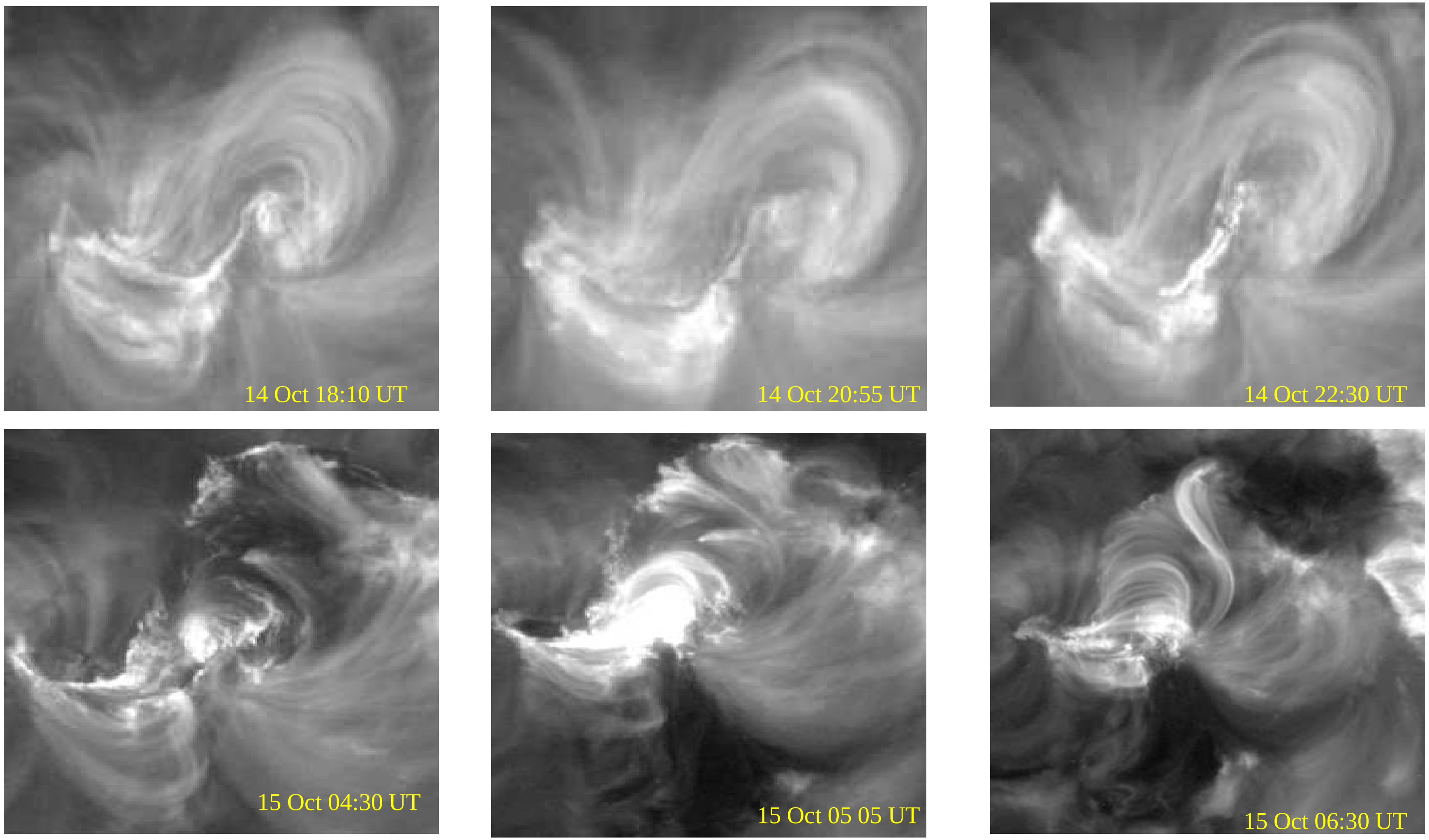

NOAA 11318: the associated CME

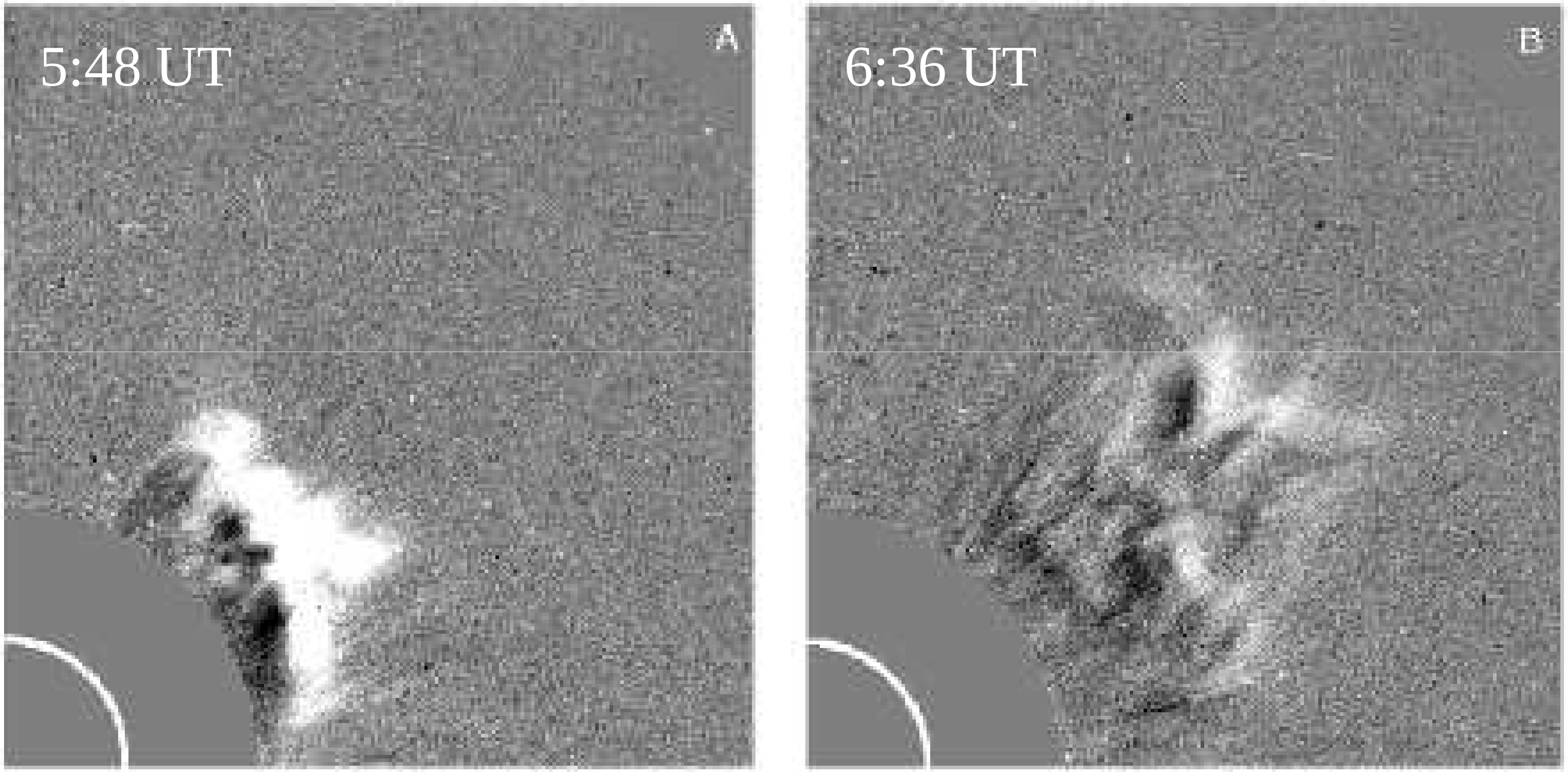

NOAA 11675

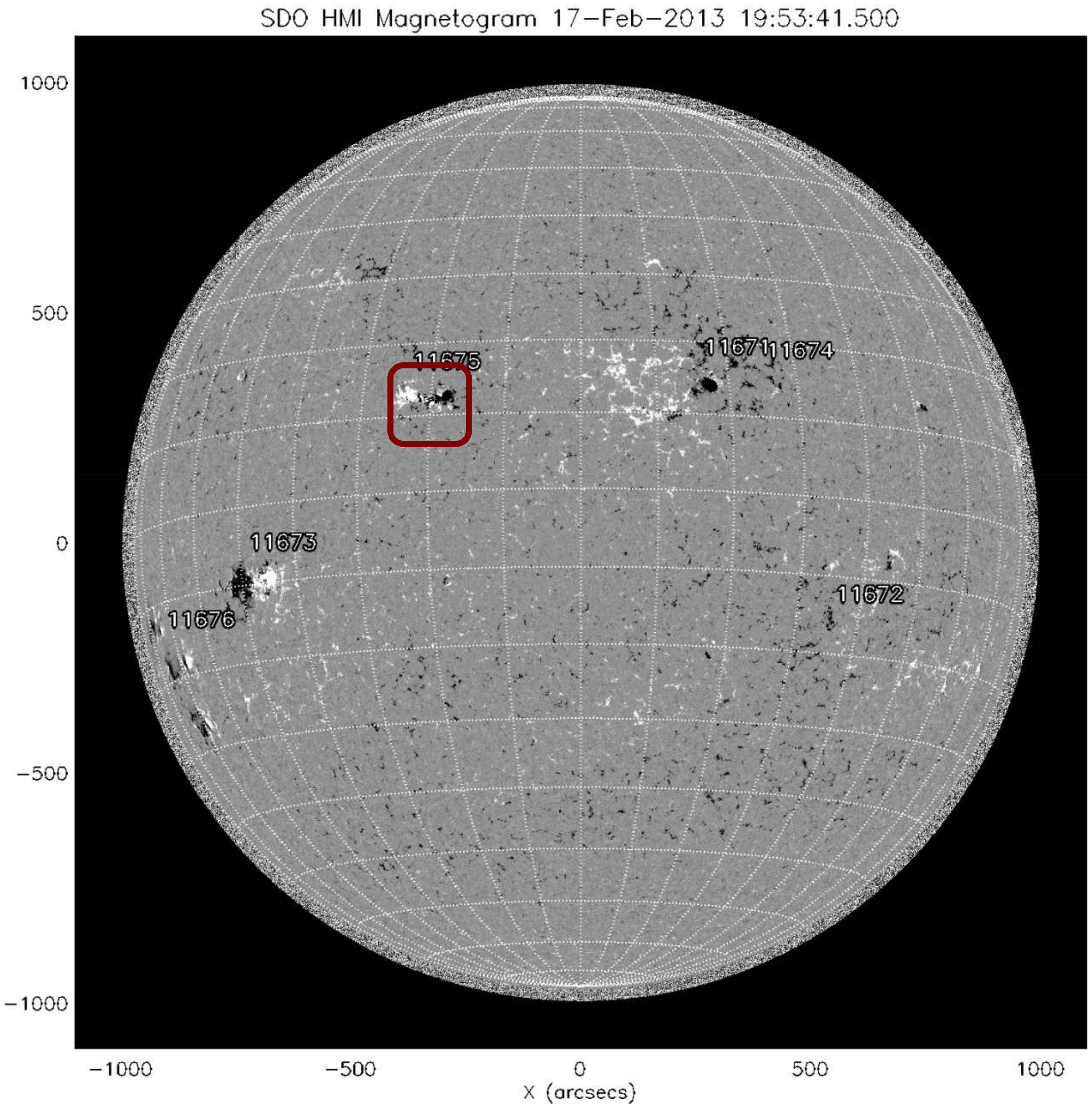

This AR has been studied using AIA/SDO and HMI/SDO longitudinal magnetograms between 16 – 21 Feb 2013

We also analyzed SDO/HMI (SHARPs) data. These data series provide maps of the photospheric vector magnetic field using VFISV code

Northern hemisphere (N12)

NOAA 11675: the magnetic field evolution

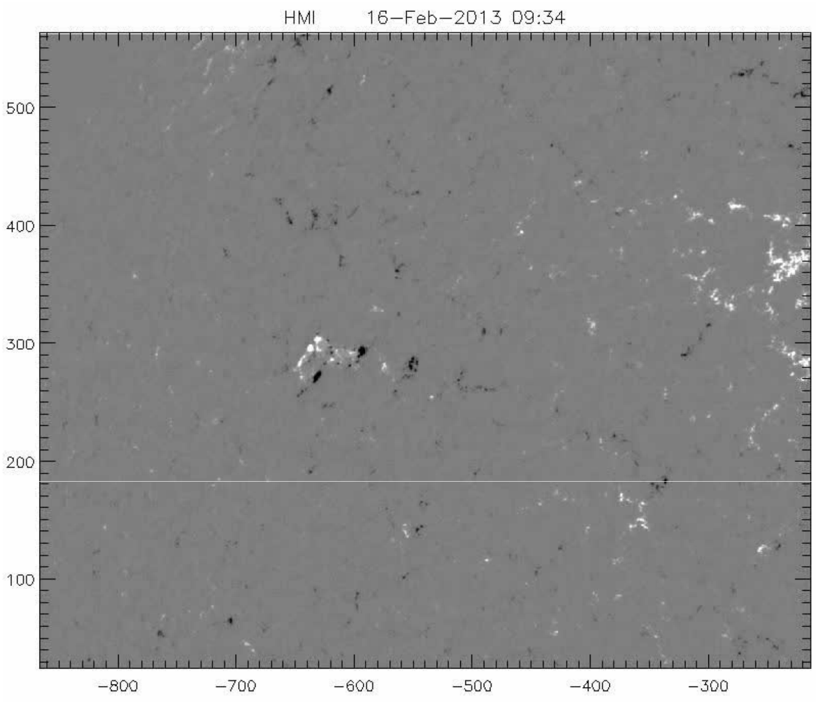

The AR shows a complex magnetic configuration, with several episodes of magnetic flux cancellation.

The continuous separation of the two polarities supports the scenario of the appearance of a flux rope.
However, in this case no sigmoid in coronal images is observed.

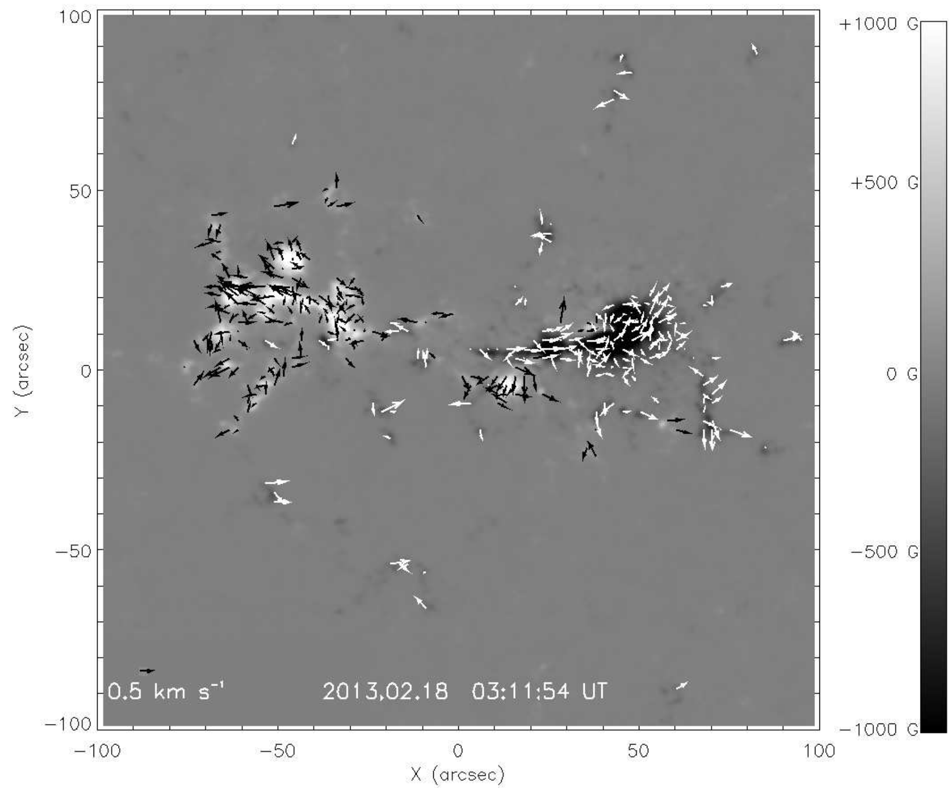

NOAA 11675: the shear angle

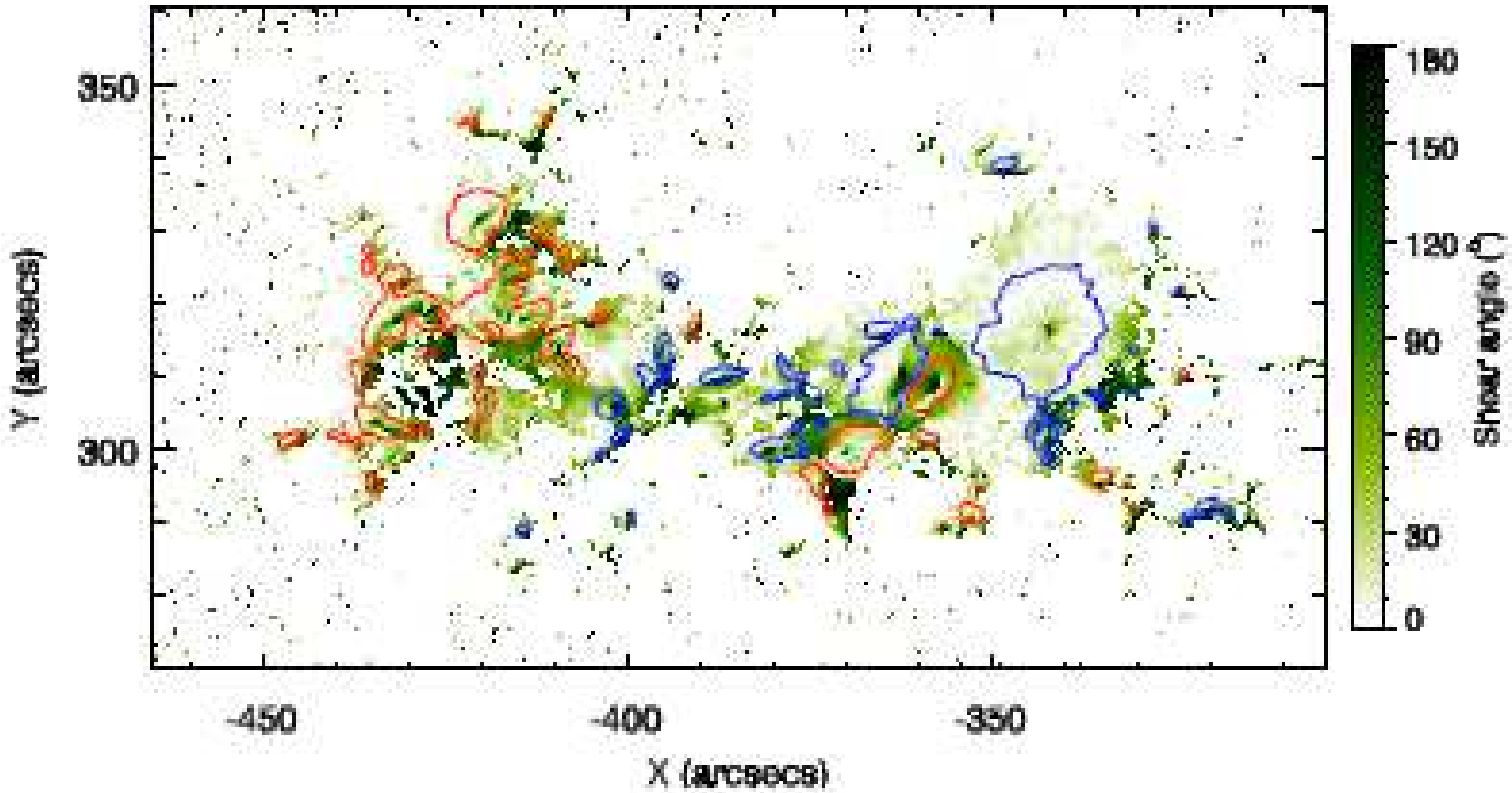

NOAA 11675 @ 304 Å

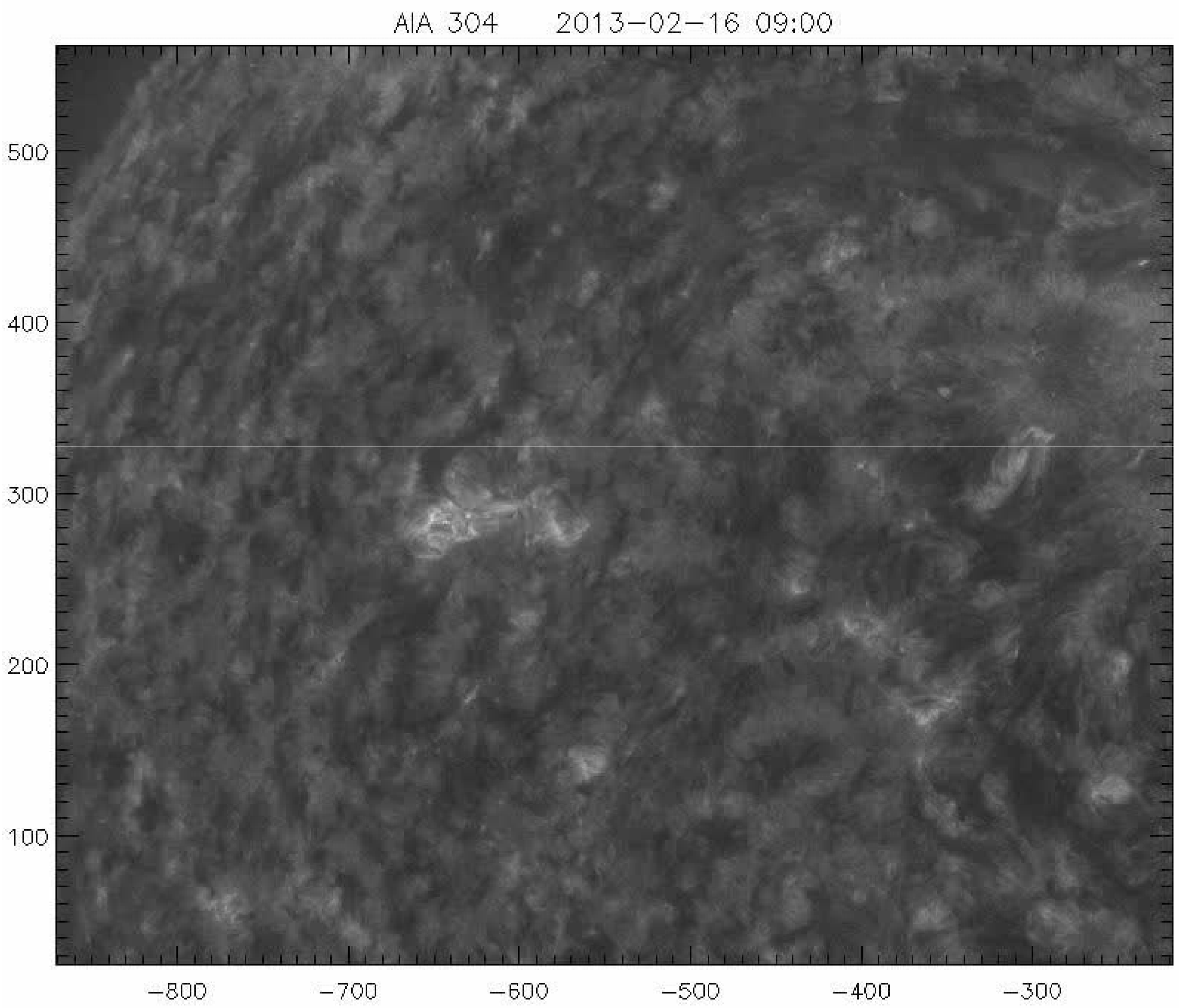

Several C class flares and one M1.9 flare are observed.

The main event occurred on 17 Feb 2013.

Forward-S shape of the filament

NOAA 11675: outflow in STEREO COR1 B

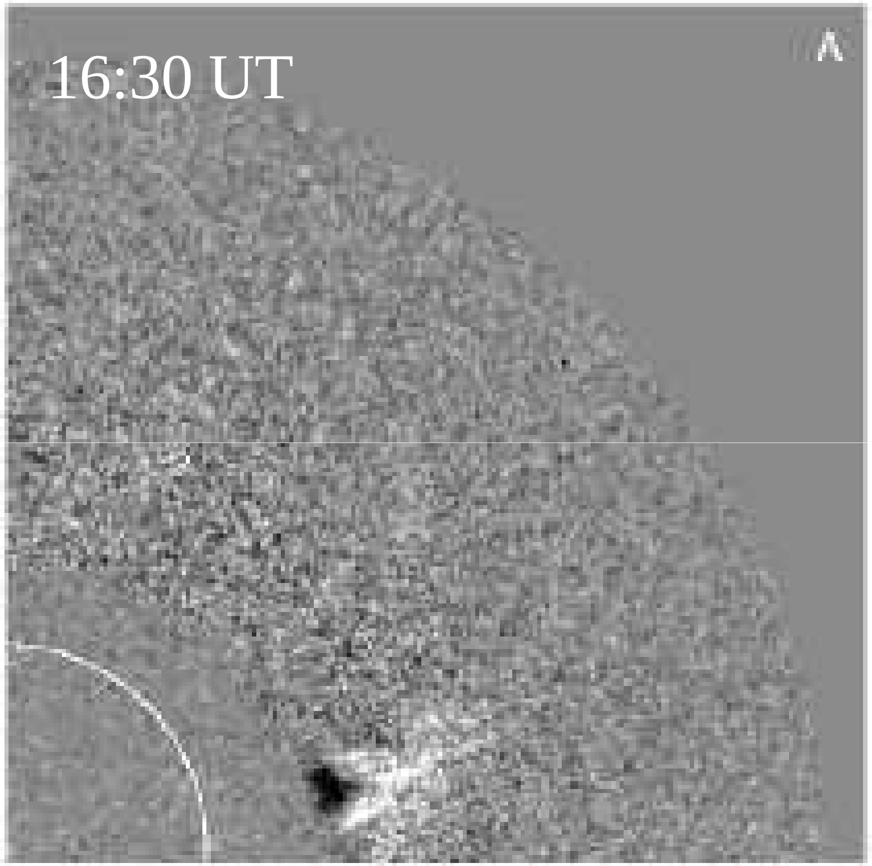

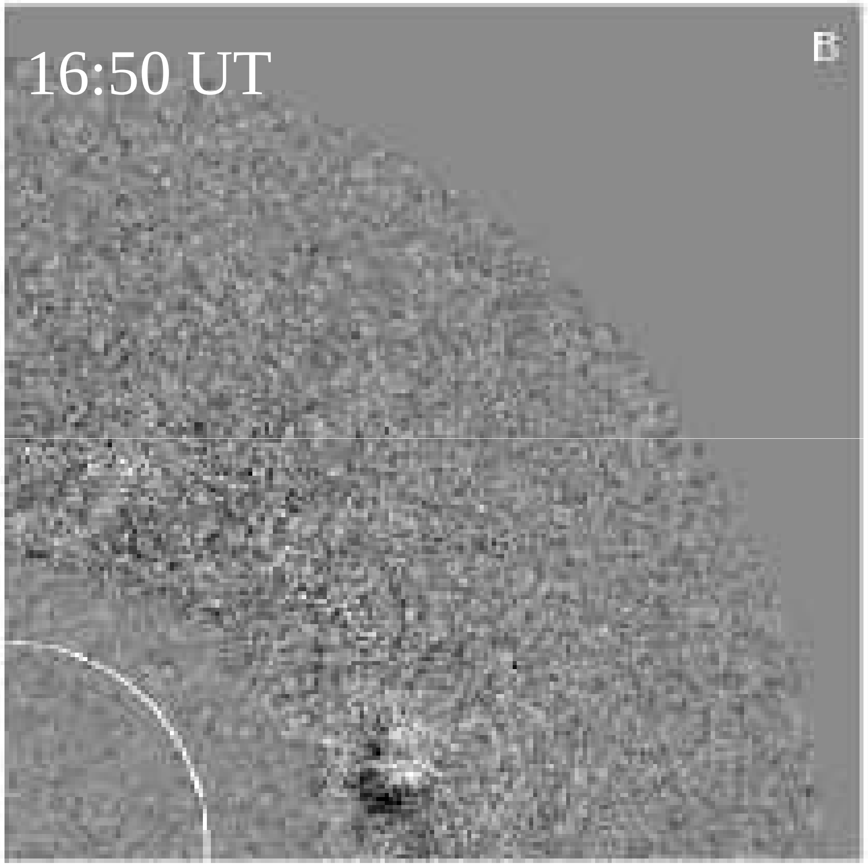

Only a minor outflow is visible in the running differences images obtained by COR1-B

Comparing the results:

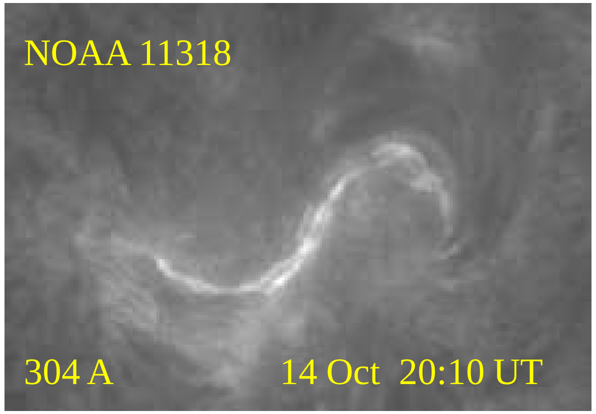

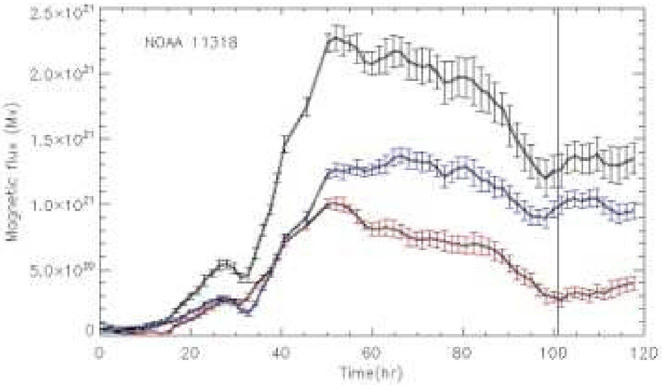

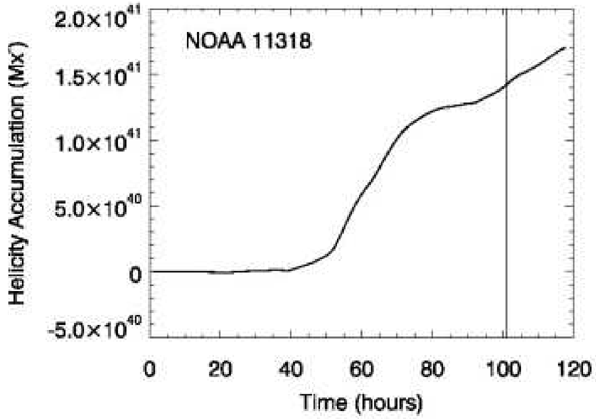

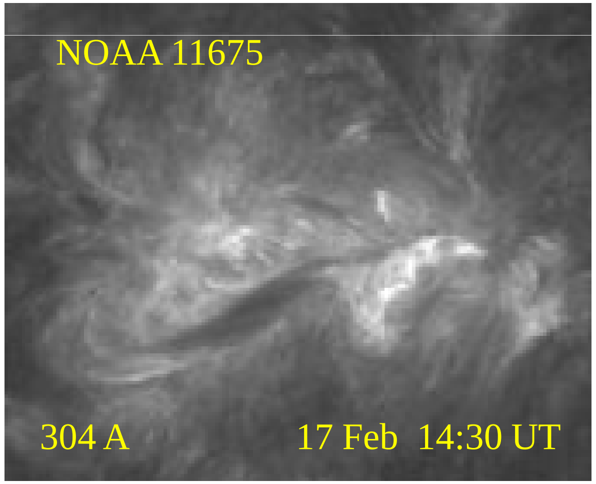

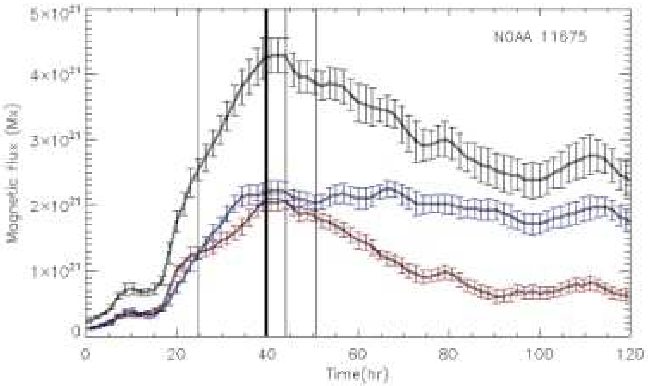

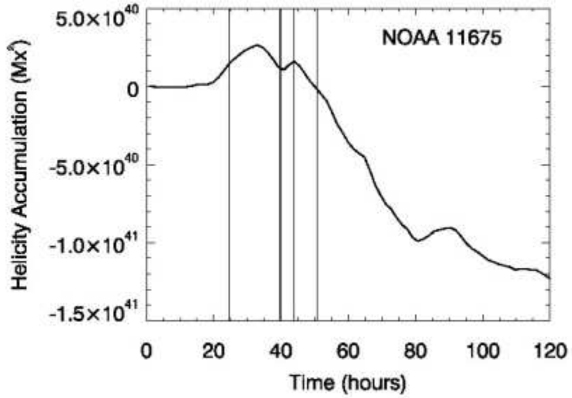

Each AR showed a different magnetic field configuration and evolution, leading to the formation of flux ropes

The sign of H does not fully obey the general cycle-invariant hemisphere helicity rule (Pevtsov et al. 1995).

Conclusions

- We detected a peculiar horizontal velocity pattern during the observation time interval of the NOAA 11283.

- The motions of the two main sunspots are responsible for the monotonic injection of positive magnetic flux.

- The shearing motions seem to be the main source of energy in corona, even if this energy is lower than the energy released by the M- and X- flares.

- The high magnetic shear and dip angle decrease after each event

- The more intense the flare is, the greater the dip and shear variations are.

The flares are powered by the energy initially present in the magnetic field system, while the shearing motions trigger its release.

Conclusions

◆The sign of the magnetic helicity is consistent with the forward-S shape sigmoid in the AR 318 and by the forward-S shape filament in the AR 675.

◆In the first case, i.e., the bipolar AR , the FR formation corresponds to a monotonic accumulation of H.

◆In the second case, we see a redistribution of H in the AR and a more complex trend of H accumulation.

◆The B- and C-class flares preceding the main event may be interpreted as signatures of magnetic reconnection processes between the forming FR and the overlying magnetic flux system that may dissipate the magnetic free energy and H from the FR into the ambient field, reducing the amount of energy available for the eruption.

Conclusions

- Both ARs accumulated more or less the same magnetic helicity amount during the same observing time interval, but only one of the ARs, the simplest one at photospheric level, produced a CME.

- Several flares occurred during the earlier phase of observations in the more complex AR, but these events did not give rise to eruptive events in the outer corona.

- We speculate that the surrounding magnetic field in the more complex AR confined the FR eruption.

For the occurrence of CMEs associated with ARs, it is important not only the presence of a FR, but also the configuration of the surrounding magnetic field
(see , i.e., Kusano et al., 2004; Galsgaard et al., 2007; Kliem & Torok 2006).

Thank you!

This research work has received funding from the European Commissions Seventh Framework Programme under the grant agreements no. 312495 (SOLARNET project) and no. 606862 (F-Chroma project). This research is also supported by the ITA MIUR-PRIN grant on “The active sun and its effects on space and Earth climate" and by Space WEather Italian COmmunity (SWICO) Research Program and by the INAF PRIN 2014.